HOMOGENEOUS BUBBLE NUCLEATION LIMIT OF LEAD

A.S. Abyzov[1]*, ***J.W.P. Schmelzer***[2], ***L.N. Davydov***[1], ***and V.V. Slezov***[1]
[1]*National Science Center "Kharkov Institute of Physics and Technology", 61108, Kharkov, Ukraine*
[2]*Institut für Physik der Universität Rostock, 18051, Rostock, Germany*

(Received October 31, 2011)

Liquid heavy metal coolant in a fast reactor, as well as in accelerator driven systems, is exhibited to large thermal and pressure shocks which can cause cavitation in the coolant. Here we calculated the work of the critical bubble formation in the lead coolant and the nucleation rate in terms of the generalized Gibbs approach. It is demonstrated that such approach provides a more adequate description of the process of bubble nucleation as compared with the classical nucleation theory.

PACS: 64.60.Qb, 72.15.Cz

1. INTRODUCTION

Liquid heavy metal heat-carrier (lead, bismuth, eutectic Pb-Bi alloy, mercury) in fast reactors and accelerator-driven reactors subject to significant thermal and hydraulic shocks. Increase in temperature and lowering of pressure (down to negative values at negative phase of a pressure wave period) can result in a cavitation in the coolant. The newly formed bubbles filled with metal vapor, together with a coolant circulation can come to the high pressure and low temperature regions, where they collapse and damage the construction materials. There are methods of controlling pressure shocks, however, temperature shocks cannot be avoided. In this paper we determine the criterions of homogeneous bubble nucleation in the liquid metal lead heat-carrier using the modified Gibbs approach [1–3] and compare the results with the classical nucleation theory (CNT).

We approached the problem in three steps. In the first step (Sec. 2), we calculated the phase equilibrium properties, the stability limit and various other properties of lead by using a slightly modified version of the equation of state [2] proposed by Redlich and Kwong [4] (see also [5–7]). In the next step (Sec. 3), we calculated the work of critical bubble formation in lead as well as the rate of homogeneous nucleation in the pressure-temperature range defined according to the results of the previous section. The paper is completed by a short summary and discussion (Sec. 4).

2. MODEL SYSTEM

For the description of lead (Pb) in both the liquid and gas phases, we will apply a slightly modified Redlich-Kwong-type equation of state as proposed by Morita et al. (see [4, 5] and, in particular, Eq. (1) in [2]). It reads

$$p=\frac{RT}{M(v-b)}-\frac{a(T)}{v(v+c)}, \qquad (1)$$

$$a(T)=a_c\,(T/T_c)^m\,, \qquad (2)$$

where $R = 8.314$ J/mol is the universal gas constant, p is pressure, v is molar volume, T is temperature, a_c, b, c and m are the model parameters specific for the substance, T_c is critical temperature.

We employ further dimensionless variables

$$\Pi\equiv\frac{p}{p_c},\ \ \omega\equiv\frac{v}{v_c},\ \ \theta\equiv\frac{T}{T_c}, \qquad (3)$$

where v_c is the molar volume, p_c the pressure both at the critical point with the critical temperature, T_c. These parameters can be determined from equation (1) in the common way via

$$\left.\frac{\partial p}{\partial v}\right|_T=\left.\frac{\partial^2 p}{\partial v^2}\right|_T=0 \quad\text{at}\quad T=T_c. \qquad (4)$$

The equation of state in reduced variables is given by

$$\Pi(\theta,\omega)=\frac{\theta}{\chi_c(\omega-\beta)}-\frac{\alpha(\theta)}{\omega(\omega+\xi)}. \qquad (5)$$

Here

$$\chi_c=\frac{p_c v_c}{RT_c} \qquad (6)$$

is the reduced critical compressibility, and

$$\alpha(\theta)=\frac{a_c\theta^m}{p_c v_c^2}=\alpha\theta^m, \qquad (7)$$

$$\beta=b/v_c,\ \ \xi=c/v_c. \qquad (8)$$

According to [6] we have then

$$\alpha=5.9,\ \ \beta=1.7\cdot10^{-3},\ \ \xi=0.768,\ \ m=-0.01. \qquad (9)$$

From equations (1) and (4) we get

$$\begin{aligned}&p_c=121\ \text{MPa},\ \rho_c=1920\ \text{kg/m}^3,\\ &v_c=5.2\cdot10^{-4}\ \text{m}^3/\text{kg},\ \ T_c=5843\ \text{K}.\end{aligned} \qquad (10)$$

---

*Corresponding author E-mail address: abyzov@kipt.kharkov.ua

The location of the classical spinodal curve can be found by the determination of the extrema of the thermal equation of state, $\Pi(\theta,\omega)$ (5), considering the temperature θ as constant. By taking the derivative of $\Pi(\theta,\omega)$ with respect to temperature, we obtain from equation (5) the result

$$\frac{\partial}{\partial\omega}\Pi(\theta,\omega)=\frac{\alpha(\theta)(2\omega+\xi)}{\omega^2(\omega+\xi)^2}-\frac{\theta}{\chi_c(\omega-\beta)^2}=0. \quad (11)$$

For $\theta<1$, this equation has two positive solutions $\omega_{\text{sp}}^{(\text{left})}$ and $\omega_{\text{sp}}^{(\text{right})}$ for ω corresponding to the specific volumes of the both macrophases at the spinodal curves (or at the limits of metastability). Similarly, the binodal curves give the values of the specific volumes of the liquid and the gas phases coexisting in thermal equilibrium at a planar interface. From the left branch of the binodal curve, we get the specific volume of the liquid phase ($\omega_l^{(\text{eq})}=\omega_{\text{b}}^{(\text{left})}$), from the right branch of the binodal curve, we obtain the specific volume of the gas ($\omega_g^{(\text{eq})}=\omega_{\text{b}}^{(\text{right})}$). For $\theta=1$, both solutions coincide in the critical point ($\omega_l^{(\text{eq})}=\omega_g^{(\text{eq})}=\omega_c=1$), again. Consequently, in order to determine the specific volumes of the liquid and the gas at some given temperature in the range $\theta\leq 1$, we have to specify the location of the binodal curve. The location of the binodal curve may be determined from the necessary thermodynamic equilibrium conditions (for planar interfaces) – equality of pressure and chemical potentials – via the solution of the set of equations

$$\Pi_l\,(\omega_l,\theta)=\Pi_g(\omega_g,\theta),\quad \mu_l(\omega_l,\theta)=\mu_g(\omega_g,\theta). \quad (12)$$

Here by μ the chemical potential of the atoms or molecules in the liquid (l) and the gas (g) are denoted. Having the equation for the reduced pressure (cf. Eq. (5)), we have now to determine in addition the chemical potential in dependence on pressure and temperature (see Sec. 2). Isotherms for lead (5) for different values of the reduced temperature $\theta=0.4, 0.65, 0.8, 0.891$ and 0.92 are shown in Fig. 1, dashed and dashed-dotted curves present the binodal and spinodal curves, correspondingly.

For isothermal processes, the change of the Helmholtz free energy, dF, may be expressed as

$$dF=-pdV+\mu dn. \quad (13)$$

Here V is the volume of the system and n the number of moles in it. For a given fixed mole number, n, of the substance ($n=const.$), we have

$$d\phi_n=-pdv,\quad \phi_n=\frac{F}{n},\quad v=\frac{V}{n}, \quad (14)$$

or, in reduced variables,

$$d\left(\frac{\phi_n}{p_cv_c}\right)=-\Pi d\omega\ . \quad (15)$$

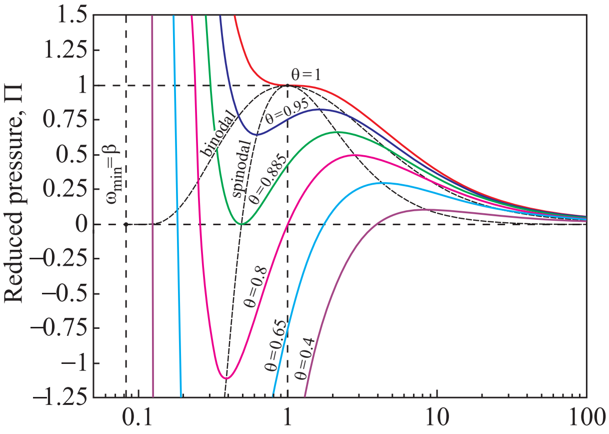

Fig. 1. *Isotherms of mercury as described via equation (5) for different values of the reduced temperature, from $\theta=0.4$ (bottom curve) to $\theta=1$ (upper curve)*

Combining equation (15) with the equation of the state, equation (5), we obtain

$$\frac{\phi_n}{p_cv_c}=-\left[\frac{\alpha(\theta)}{\xi}\ln\left(\frac{\xi}{\omega}+1\right)+\frac{\theta\cdot\ln(\omega-\beta)}{\chi_c}\right]. \quad (16)$$

Alternatively, the isochoric change of the Helmholtz free energy is given at constant temperature by

$$dF=\mu dn. \quad (17)$$

From equation (17),

$$d\phi_v=-\frac{\mu}{v^2}dv,\quad \phi_v=\frac{F}{V}\ . \quad (18)$$

On the other side, the functions $d\phi_v$ and ϕ_n are connected by

$$F=\phi_n n=\phi_v V,\quad \phi_v=\frac{\phi_n}{v}\ . \quad (19)$$

With equation (16), we have then

$$\phi_v=\frac{p_c}{\omega}\left[\frac{\alpha(\theta)}{\xi}\ln\left(\frac{\xi}{\omega}+1\right)+\frac{\theta\cdot\ln(\omega-\beta)}{\chi_c}\right]. \quad (20)$$

With equations (18) and (20), the expression for the chemical potential of a heavy liquid metal (HLM) can be obtained then via

$$\mu=-v^2\frac{\partial\phi_v}{\partial v}=-v_e\omega^2\frac{\partial\phi_v}{\partial v}\ . \quad (21)$$

This relation yields

$$\begin{aligned}\frac{\mu(\omega,\theta)}{p_cv_c}=-\Big[\frac{\alpha(\theta)}{\omega+\xi}+\frac{\theta\cdot\omega}{\chi_c(\beta-\omega)}+\\ +\frac{\alpha(\theta)}{\xi}\ln\left(\frac{\xi}{\omega}+1\right)+\frac{\theta\cdot\ln(\omega-\beta)}{\chi_c}\Big]+\psi(\theta)\ .\end{aligned} \quad (22)$$

In addition to the bulk properties of the system, we have to know the value of the surface tension, σ, for planar interfaces in dependence on the parameters describing the state of both phases. The following form was chosen for our calculation [3, 8–10]

$$\sigma(\omega_g,\omega_l,\theta)=\Theta(\theta)\left[\frac{1}{\omega_l}-\frac{1}{\omega_g}\right]^{\delta}, \quad (23)$$

where

$$\Theta(\theta) = A\left[\frac{1}{\omega_{\mathrm{b}}^{(\mathrm{left})}} - \frac{1}{\omega_{\mathrm{b}}^{(\mathrm{right})}}\right]^{k-\delta}, \quad \delta = 2, \qquad (24)$$

and A and k are constant parameters. Comparison of equations (23) and (24) with experimental data [11, 12]

$$\sigma(T) = 0.4857 - 0.000066 \cdot T \qquad (25)$$

(valid in this form only for temperatures far below the critical temperature; here the temperature is given in Kelvin and the surface tension in $\mathrm{J/m^2}$) at $\omega_l = \omega_{\mathrm{b}}^{(\mathrm{left})}$ and $\omega_g = \omega_{\mathrm{b}}^{(\mathrm{right})}$ yields

$$A = \ 40.5 \cdot 10^{-3}\ \mathrm{J/m^2}, \quad k = 1.4. \qquad (26)$$

3. DETERMINATION OF THE WORK OF CRITICAL CLUSTER FORMATION

Let us assume that the system is brought suddenly into a metastable state located between binodal curve and spinodal curve on the liquid side. Then, by nucleation and growth processes, bubbles may appear spontaneously in the liquid and a phase separation takes place [13]. Based on the relations outlined above, we will find the temperature and pressure dependence of the parameters of the critical vapour cluster formation. We start with the general expression for the change of the thermodynamic potential

$$\Delta G = \sigma A + (p - p_\alpha)V_\alpha + \sum_j n_{j\alpha}(\mu_{j\alpha} - \mu_{j\beta})\ . \qquad (27)$$

Here the subscript α specifies the parameters of the cluster (bubble) phase while β refers to the ambient liquid phase. This relation holds as long as the state of the liquid remains unchanged by the formation of one bubble. For a one-component system, this expression is reduced to

$$\Delta G = \sigma A + (p - p_\alpha)V_\alpha + n_\alpha(\mu_\alpha - \mu_\beta)\ . \qquad (28)$$

As independent variables, we selected the radius of the bubble, r, and the molar volume of the gas phase in the bubble. Similarly to [2, 3, 14] we arrive then at

$$\frac{\Delta g(r, \omega_g, \omega_l, \theta)}{k_B T} = 3\left(\frac{1}{\omega_l} - \frac{1}{\omega_g}\right)^{\delta} r^2 + 2f(\omega_g, \omega_l, \theta) r^3\ , \qquad (29)$$

where the following notations have been introduced:

$$\begin{aligned} f(\omega_g, \omega_l, \theta) &= \Pi(\omega_g, \theta) - \Pi(\omega_l, \theta) + \\ &+ (\omega_g p_c v_c)^{-1}\left(\mu(\omega_l, \theta) - \mu(\omega_g, \theta)\right), \end{aligned} \qquad (30)$$

$$g \equiv \frac{G}{\Omega_1}, \quad \Omega_1 = \frac{16\pi}{3}\frac{1}{p_c^2 k_B T_c \theta}\Theta^3(\theta)\ , \qquad (31)$$

$$r \equiv \frac{R}{R_\sigma}, \quad R_\sigma = \frac{2}{p_c}\Theta(\theta). \qquad (32)$$

The Gibbs free energy surface for the metastable initial state has a typical saddle shape near to the configuration corresponding to a bubble of critical size (see Fig. 2, $\theta = 0.75$, $\Omega_1 = 0.44$) in the space of critical radius-molar volume and work of cluster formation.

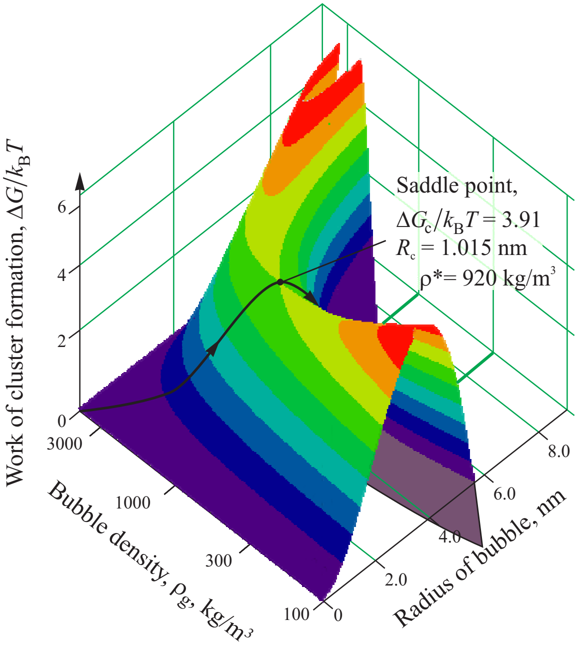

Fig. 2. *Gibbs free energy surface for metastable initial state, $\theta = 0.75$, $\Omega_1 = 0.44$*

The critical point position is determined by the following set of equations

$$\frac{\partial \Delta g(r, \omega_g, \omega_l, \theta)}{\partial r} = 0, \quad \frac{\partial \Delta g(r, \omega_g, \omega_l, \theta)}{\partial \omega_g} = 0. \qquad (33)$$

The dependence of the critical cluster parameters on the negative pressure, p, are shown in Figures 3-5, for $\theta = 0.70$. The positions of the binodal and spinodal curves are given then by $\omega_{\mathrm{b}}^{(\mathrm{left})} = 0.311$, $p_{\mathrm{b}} = -0.254$, and $\omega_{\mathrm{sp}}^{(\mathrm{left})} = 0.44$, $p_{\mathrm{sp}} = 1.174$, correspondingly. $p_{\mathrm{sp}} = 1.812$.

Compare the obtained results with the classical nucleation theory (CNT). The work of formation of critical nucleus $\Delta G_{\mathrm{class}}$ is determined in this case by the following equation (see, for example, [13])

$$\frac{\Delta G_{\mathrm{class}}}{k_B T} = \frac{16\pi}{3}\frac{\sigma^3}{(p - p_g)^2 k_B T}. \qquad (34)$$

Fig. 3 presents the dependence of gas density in critical nucleus on the density of liquid. Close to binodal (at very small metastability) the density of gas in a bubble only insignificantly differs from its equilibrium value (the same as in CNT). However, as the metastability increases the gas density in a bubble grows, coming closer to the density of the surrounding liquid taken at spinodal. At the same time (see Eq. (23)) the bubble surface energy decreases, and, correspondingly, the work of nucleus formation also decreases.

The dependence of the work of critical nucleus formation $\Delta G_c/k_B T$, on negative pressure in a generalized Gibbs model (blue line) and CNT (green line) is shown in Fig. 4. It is evident that in CNT the work of critical nucleus formation does not “feel” spinodal, while for in the generalized Gibbs model the work decreases with the approach to spinodal. Indeed, at spinodal the gas density in a bubble coincides with the density of the liquid (see Fig. 3). It means, that such “nucleus” does not differ from a surrounding it medium and, naturally, the work of its formation is equal to zero. Therefore, the nucleation process close to spinodal goes not through a saddle point, but through a ridge of the potential ΔG (in details see [15]).

The behaviour of the critical radius with the approach to the binodal also differs in these theories: in the generalized Gibbs model the critical radius sharply increases (however, this does not influence the nucleation: as was mentioned above, the nucleation process close to spinodal does not pass through the saddle point), and in CNT there is no singularity (Fig. 5).

The nucleation rate is determined by the following equation

$$I = I_0 \exp\left(-\frac{\Delta G_c}{k_B T}\right) . \tag{35}$$

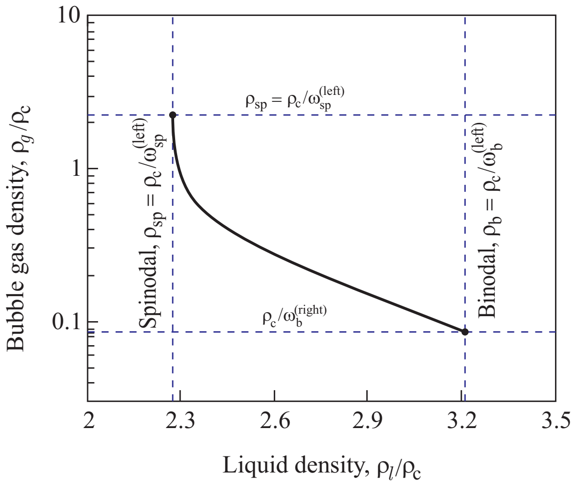

Fig. 3. *Dependence of gas density in the bubble on liquid density*

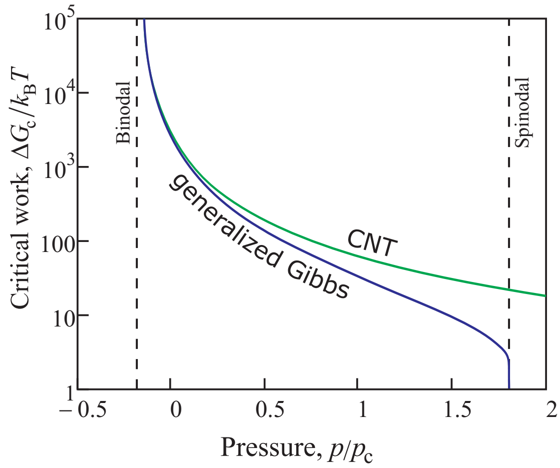

Fig. 4. *Dependence of work of the critical bubble formation, $\Delta G_c/k_\mathrm{B}T$, on negative pressure*

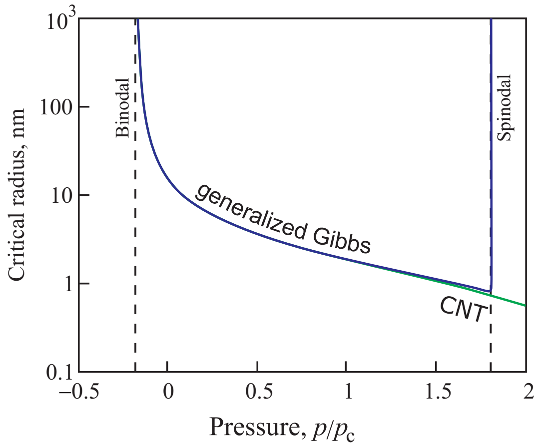

Fig. 5. *Dependence of the radius of the critical bubble, R_c, on negative pressure*

Fig. 6 presents the dependence of the nucleation rate on negative pressure in the generalized Gibbs model (blue) and CNT (green) (in calculation the preexponential factor equaled $I_0 \approx 10^{41}\,\mathrm{m}^{-3}\,\mathrm{s}^{-1}$). It is evident that the nucleation rate calculated in the classical theory is several orders less than the generalized Gibbs model predicts.

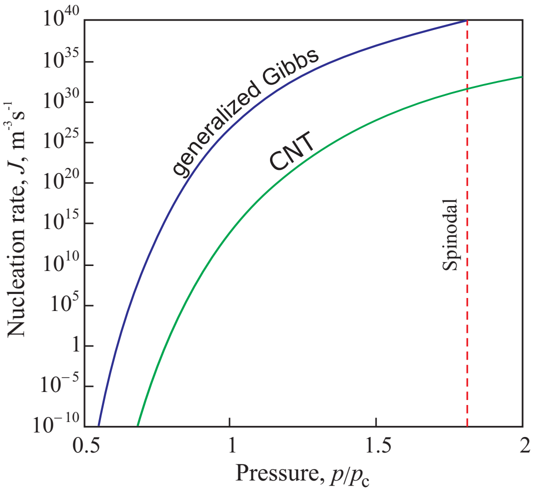

Fig. 6. *Dependence of nucleation rate J on negative pressure*

4. CONCLUSIONS

Near the binodal the generalized Gibbs approach leads to the same results as the classical nucleation theory, but noticeably different ones for enough large degree of metastability, that is close to the spinodal (see Figs. 7, 10 and [1, 3, 14]). Therefore, the considered approach is of importance for cavitational processes, which take place mainly at large metastability. It was found that the nucleation rate, calculated within the generalized Gibbs model is several orders higher than the classical theory predicts, that is the limit of cavitational stability is noticeably lower than in the classical theory. Note that the calculations were done only for the case of homogeneous bubble nucleation in the coolant bulk. However, the heterogeneous nucleation at impurities in the coolant or on the pipelines walls is also possible. The work of formation of critical bubbles is in this case lower, but also the number of nucleation sites is much less, therefore the influence of heterogeneous nucleation on the threshold of cavitational stability requires additional investigation.

References

1. V.V. Slezov. *Kinetics of First-Order Phase Transitions.* Weinheim: "Wiley-VCH Publishers", 2009, 429 p.
2. A.R. Imre, A.S. Abyzov, I.F. Barna, and J.W.P. Schmelzer. Homogeneous bubble nucleation limit of mercury under the normal working conditions of the planned European spallation neutron source // *Eur. Phys. J.* 2011, v. B79, p. 107-113.
3. J.W.P. Schmelzer, J. Schmelzer, Jr. Kinetics of bubble formation and the tensile strength of liquids // *Atmospheric Research.* 2003, v. 65, p. 303-324.
4. O. Redlich, J.N.S. Kwong. On the Thermodynamics of Solutions. V. An Equation of State. Fugacities of Gaseous Solutions // *Chem. Rev.* 1949, v. 44, p. 233-244.
5. K. Morita, W. Maschek, M. Flad, Y. Tobita, H. Yamano. Critical parameters and equation of state for heavy liquid metals // *J. Nucl. Sci. Technol.* 2006, v. 43, p. 526-537.
6. K. Morita, V. Sobolev, M. Flad. Critical parameters and equation of state for heavy liquid metals // *J. Nucl. Mat.* 2007, v. 362, p. 227-234.
7. K. Morita, E.A. Fischer. Thermodynamic properties and equations of state for fast reactor safety analysis. Part I: Analytic equation-of-state model // *Nucl. Eng. Des.* 1998, v. 183, p. 177-191.
8. J.D. van der Waals, Ph. Kohnstamm. *Lehrbuch der Thermodynamik.* Leipzig und Amsterdam: "Johann-Ambrosius-Barth Verlag", 1908, 646 p.
9. K. Binder. Spinodal Decomposition // *Materials Science and Technology* / Edited by R.W. Cahn, P. Haasen, E.J. Kramer. Weinheim: "VCH", 1991, v. 5, p. 405.
10. D.B. Macleod. On a relation between surface tension and density // *Trans. Faraday Soc.* 1923, v. 19, p. 38-41.
11. B.B. Alchagirov and A.G. Mozgovoi. Experimental Investigation of the Surface Tension of Liquid Lead and Bismuth in the Vicinity of the Melting Point // *High Temperature.* 2003, v. 41, p. 412-414.
12. A.E. Schwaneke, W.L. Falke. Surface tension and density of liquid lead // *J. Chem. Eng. Data.* 1972, v. 17(3), p. 291-293.
13. V.P. Skripov. *Metastable Liquids.* New York: "Wiley", 1974, 272 p.
14. A.S. Abyzov, J.W.P. Schmelzer. Nucleation versus spinodal decomposition in confined binary solutions // *J. Chem. Phys.* 2007, v. 127, 114504.
15. A.S. Abyzov, J.W.P. Schmelzer, A.A. Kovalchuk, V.V. Slezov. Evolution of Cluster Size-Distributions in Nucleation-Growth and Spinodal Decomposition Processes in a Regular Solution // *J. Non-Cryst. Solids.* 2010, v. 356, p. 2915.

ПОРОГ ГОМОГЕННОГО ЗАРОЖДЕНИЯ ПУЗЫРЬКОВ В СВИНЦЕ

А.С. Абызов, Ю.В.П. Шмельцер, Л.Н. Давыдов, В.В. Слёзов

Теплоносители на основе жидких тяжелых металлов в быстрых реакторах и реакторах, управляемых ускорителем, подвержены значительным тепловым и гидравлическим ударам, что может приводить к кавитации теплоносителя. Рассчитаны работа образования критических пузырьков в свинцовом теплоносителе и скорость их зарождения в рамках обобщенного подхода Гиббса. Показано, что такой подход обеспечивает более адекватное описание процесса зарождения пузырьков по сравнению с классической теорией нуклеации.

ПОРІГ ГОМОГЕННОГО ЗАРОДЖЕННЯ ПУХИРЦІВ У СВИНЦІ

О.С. Абизов, Ю.В.П. Шмельцер, Л.М. Давидов, В.В. Сльозов

Теплоносії на основі рідких важких металів у швидких реакторах і реакторах, керованих прискорювачем, схильні до значних теплових і гідравлічних ударів, що може призводити до кавітації теплоносія. Розраховані робота утворення критичних пухирців в свинцевому теплоносії та швидкість їх зародження в рамках узагальненого підходу Гіббса. Показано, що такий підхід забезпечує більш адекватний опис процесу зародження пухирців в порівнянні з класичною теорією нуклеації.